Risk Assessment of Water Inrush in Coal Seam Floor Based on a Dynamic Variable Weight Model and 3D Probability Space Comparison

Yanlei Li[1], Bin Zhang[1], Tao Wu[1], Yongjie Li[2, 3, *], Shuzhen Tai[2, 3], Guoliang Xu[4], Fangying Dong[2, 3], Huiyong Yin[2, 3]

[1]Binhu Coal Mine, Zaozhuang Mining (Group Co., Ltd.), Zaozhuang 277599, China
[2]Shandong University of Science and Technology, Qingdao 266590, China
[3]State Key Laboratory of Disaster Prevention and Ecology Protection in Open-pit Coal Mines, Qingdao 266590, China
[4]Geophysical Survey Team of Shandong Coal Geology Bureau, Jinan 250100, China

Abstract: Mining under the Ordovician limestone aquifer is severely threatened by coal seam floor water inrush, which endangers mining safety. Traditional fixed-weight evaluation models for coal floor water inrush risk have prominent limitations: they ignore the internal variability among index values, easily distorting prediction results and failing to meet the demand for accurate risk assessment. To address this issue, this study proposes a dynamic variable weight evaluation model for coal floor water inrush risk based on the Improved Fuzzy Analytic Hierarchy Process (IFAHP) and Entropy Weight Method (EWM). First, after comprehensive analysis of hydrogeological data, six key evaluation indicators were selected, including Ordovician limestone water pressure, Ordovician limestone water abundance, aquifuge thickness, fragile rock ratio, fault fractal dimension, and floor failure depth. Subjective weights from IFAHP and objective weights from EWM were then combined to obtain comprehensive weights. Subsequently, the K-means algorithm was applied for unified clustering analysis of the indices to define variable weight intervals and construct the dynamic variable weight model. Based on this model, ArcGIS was used to classify Ordovician limestone water inrush risk into four levels and generate a risk zoning map for the 16th coal seam floor. Validation with known water inrush points and comparative analysis with the constant-weight model demonstrated that the proposed IFAHP-EWM dynamic variable weight method has higher prediction accuracy and better spatial adaptability. Additionally, 3D visualization of the risk zoning map was developed to enhance practical application. This model provides a reliable theoretical basis and practical tool for improving the safety of coal seam floor mining under Ordovician limestone aquifers.

Keywords: Water Inrush Risk Assessment; Improved Fuzzy Analytic Hierarchy Process; Entropy Weight Method; Dynamic Variable Weight; K-means Clustering

DOI: 10.57237/j.wjese.2026.01.001

1 Introduction

Water inrush from the Ordovician limestone aquifer poses a major hazard to coal mine safety in the North China Coalfield [1]. The Carboniferous-Permian coal seams are underlain by a thick, high-pressure Ordovician limestone aquifer with strong water yield and recharge capacity, making depressurization measures difficult to implement [2]. More than 230 mines in this region are threatened by Ordovician water, affecting over 14.97 billion tons of coal reserves [3]. There-

[*]Corresponding author: Yongjie Li, yongjie.li@sdust.edu.cn

Received: 28 November 2025; Accepted: 29 December 2025; Published Online: 20 January 2026

fore, accurate assessment and prevention of floor water inrush are essential for safe resource extraction.

Traditional evaluation approaches—such as the water inrush coefficient method, hydrogeological analysis, and geophysical exploration—provide useful information but are often costly, data-intensive, and limited by single-factor or static analysis [4]. Multi-factor evaluation models have shown improved reliability. For instance, Wu [5] applied GIS-based indices and AHP; Hou [6] adopted an improved AHP-EWM model; Shi [7] used a Grey Wolf Optimized neural network; and Li [8] developed comprehensive evaluation and PCA-TOPSIS frameworks. Additional studies incorporating hydrochemical analysis and fault complexity have further advanced understanding of inrush mechanisms [9].

However, most existing models rely on constant weighting schemes that do not account for spatial heterogeneity or variations in indicator significance, potentially leading to oversimplified assessments and weight subjectivity [10]. To address these limitations, this study develops a dynamic variable-weight model that integrates subjective weights from the Improved Fuzzy Analytic Hierarchy Process (IFAHP) with objective weights from the Entropy Weight Method (EWM). K-means clustering is used to establish adaptive weight adjustment intervals, enabling indicator weights to vary according to geological conditions.

The model is applied to the Binhu Coal Mine (BHCM) in Shandong Province, where multiple water inrush events have occurred in the 16th coal seam, especially in panels 216 and 316. Using six key geological and hydrogeological indicators, the proposed framework improves prediction accuracy and provides a practical basis for risk prevention in mining operations.

2 Overview of the Study Area

BHCM is located in Binhu Town, Tengzhou City, within the central-western Tengbei mining district of Shandong Province, approximately 20 km west of downtown Tengzhou. The mine comprises four mining zones and is dominated by a northwest-dipping monocline with minor short-axis folds. Faults are well developed, mainly NE-trending and nearly N-S-trending normal faults and NE-trending reverse faults, with throws of 5-50 m.

The aquifer system shows clear vertical stratification. Quaternary aquifers thin from west to east, while the underlying Ordovician limestone aquifer lies 36.62-66.52 m below the 16th coal seam and shows no floor heave. Borehole results indicate minimal fault-related inflow, reflecting good cementation and low permeability. Regionally, shallow aquifers in adjacent mines are dewatered in advance to reduce pressure.

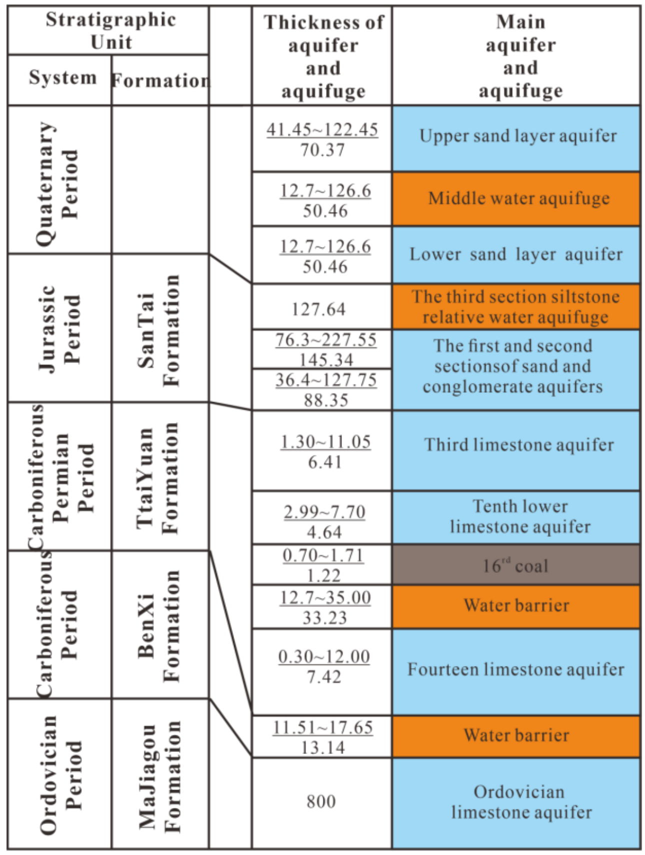

Figure 1 Comprehensive stratigraphic column diagram of the study area

From top to bottom, the hydrogeological units include a Quaternary sand aquifer, a Quaternary aquitard, Jurassic sandstone-conglomerate aquifers, Taiyuan Formation limestones, and the Ordovician limestone (Figure 1). The 10th limestone is the direct water-bearing horizon but has low yield, whereas the 14th limestone and the Ordovician aquifer provide indirect recharge. Due to its high pressure and large storage capacity, the Ordovician limestone is the principal source controlling floor water-inrush risk.

3 Index Selection and Data Standardization

A range of factors affect the probability of water inrush from the coal seam floor, such as the study area’s geological conditions, hydrogeological properties, and the degree of previous exploration [11]. Drawing on field surveys, published studies, and earlier research findings, six core indicators were chosen to build the evaluation index system (Figure 2).

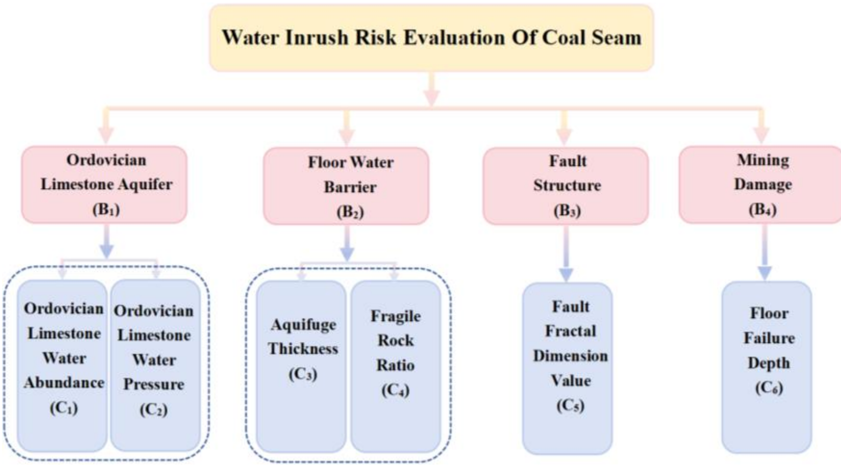

Figure 2 Structural model of floor water risk assessment index

3.1 Aquifer Water Pressure (AWP)

The underlying aquifer pressure applies hydrostatic and hydrodynamic stresses to the floor aquiclude, weakening its water-resisting capacity and providing the key driving force for confined water to migrate into the mining face. Once mining disturbs potential flow paths, this pressure accelerates the development of seepage channels. Moreover, when aquifer pressure is sufficiently high, floor water inrush may occur even without significant mining-induced damage or new hydraulic connections [12], as shown in Figure 3a.

The mathematical expression for calculating aquifer water pressure is presented in Eq. (1):

$$P = \rho g(h_1 - h_2) \tag{1}$$

Where, P is the water pressure, MPa; ρ is the water density, kg/m^3; g is gravitational acceleration, N/kg; h_1 is the aquifer water level elevation, m; h_2 is the aquifuge floor elevation, m.

3.2 Aquifer Water Abundance (AWA)

Aquifer water abundance provides the fundamental water source for inrush events and determines the severity of potential inflow. It reflects the aquifer's storage and discharge capacity; higher abundance indicates greater inrush likelihood. It is mainly controlled by hydrogeological conditions, lithology, structural integrity, and recharge. Practically, it is characterized using indicators such as spring discharge, well yield, unit inflow, permeability coefficient, and groundwater runoff modulus (Figure 3b).

3.3 Aquifuge Thickness (AT)

Aquifuge thickness refers to the vertical distance between the coal seam floor and the upper boundary of the Ordovician limestone aquifer. It is one of the most direct indicators of water-resisting capacity: a thicker aquifuge better prevents confined water from penetrating upward and enhances roadway stability. Therefore, accurately determining aquifuge thickness is vital for evaluating and preventing water inrush risk (Figure 3c).

3.4 Fragile Rock Ratio (FRR)

Different lithologies within the aquifuge respond differently to mining stress. Brittle rocks are prone to fracture, forming joints that increase permeability and water migration, while hard rocks maintain stability and plastic rocks deform without significant cracking. Thus, the proportion of brittle rock determines the aquifuge's sealing performance [13]. Evaluating lithologic composition and brittle layer thickness is key to assessing floor water-resisting capacity (Figure 3d).

3.5 Fault Fractal Dimension Value (FFDV)

Faults act as preferential channels for groundwater, and their scale and connectivity significantly influence water inrush. The fault fractal dimension integrates multiple fault parameters into a quantitative index. Based on mine coordinates, the area is divided into grids (200 × 200 m to 25 × 25 m), fault traces are counted, and fractal dimensions are calculated via logarithmic regression [14] (Figure 3e).

3.6 Floor Failure Depth (FFD)

Mining-induced stress causes fracturing in the coal seam floor, forming a failure zone that may connect with the aquifer. The risk of water inrush is controlled by aquifuge thickness and integrity. A thinner or disrupted aquifuge increases hydraulic connectivity. Under relatively uniform geological conditions, floor failure and inrush risk can be analyzed using thin plate and fixed beam theory (Figure 3f).

3.7 Data Standardization

To eliminate the dimensional inconsistencies among different indicators during the superposition process, the original data were normalized using the range standardization method (Eq. (2)).

$$Z_i = \frac{x_i - \min(x_i)}{\max(x_i) - \min(x_i)} \tag{2}$$

where, Z_i is the raw index value; $\max(x_i)$ denotes the maximum; $\min(x_i)$ is the minimum value in the original data.

3.8 Data Analysis

Correlation analysis of the six control indicators is presented in Table 1. AWA and AWP show a strong positive correlation at the 1% significance level (r = 0.799), indicating that areas with greater water abundance generally exhibit higher water pressure, thereby increasing the driving force and likelihood of water inrush. Meanwhile, AWA is significantly negatively correlated with FFD, suggesting that well-developed faults reduce aquifer storage, as groundwater preferentially migrates along fault zones rather than remaining in limestone pores. AWP also shows a significant positive correlation with FFD, implying that faulted zones are conducive to the accumulation of high-pressure water, which favors the formation of inrush pathways.

AT exhibits a moderate positive correlation with AWP, while correlations with other indicators are not significant, indicating that its hydraulic isolation effect is strongly influenced by regional geological structures. Additionally, FFDV is significantly positively correlated with FFD, demonstrating spatial consistency between fault complexity and development intensity. Thus, these two indicators should be jointly considered when assessing and preventing water inrush hazards.

Table 1 Correlation analysis

	AWA	AWP	AT	FRR	FFDV	FFD
AWA	1					
AWP	0.799**	1				
AT	0.071**	0.395**	1			
FRR	0.177**	-0.156**	-0.087**	1		
FFDV	0.136**	-0.146**	-0.004	0.045*	1	
FFD	-0.659**	0.652**	0.088**	0.083**	0.213**	1

Notes: ** and * represent a significance level of 1% and 5% respectively.

4 Weight Determination Using IFAHP and EWM

4.1 The Subjective Weights Is Determined by IFAHP

The weight of each index represents the relative contribution or significance of the influencing factors [15]. In this study, the Improved Fuzzy Analytic Hierarchy Process (IFAHP) is applied to determine the subjective weight. Compared with the traditional analytic hierarchy method, IFAHP not only aligns with human logical judgment but also provides a simpler and more precise form for multi-objective decision analysis [16]. It has notable advantages, such as faster consistency checking of the judgment matrix, higher computational accuracy, and quicker convergence, which make the results more consistent with actual conditions [17].

Table 2 0.1~0.9 Quantity scale

Scale	Compare	Definition
0.5	equal importance	A and B are considered to have the same level of importance
0.6	Slight importance	A is judged to be slightly more important than B
0.7	Clear importance	A is judged to be more important than B to a clear extent
0.8	strong importance	A is judged to be much more important than B
0.9	Extreme importance	A is judged to be extremely more important than B
0.1, 0.2, 0.3, 0.4	Reciprocal values	Indicates that the elements a and b are compared to obtain and then the elements and elements are judged by comparison to obtain

1) To characterize the relative influence between any pair of factors under a given criterion, the 0.1-0.9 scaling method (Table 2) is employed, based on which the priority judgment matrix is constructed.

$$F=\left(f_{ij}\right)_{n\times n} \tag{3}$$

2) Obtain the row and Eq. (4), and transform Eq. (1) into fuzzy consistency judgment matrix Eq. (6), by using transformation Eq. (5).

$$\mathrm{r_i}=\sum_{j=1}^{n} f_{ij} \tag{4}$$

$$r_{ij}=\frac{r_i-r_j}{2n}+0.5 \tag{5}$$

$$R=\left(r_{ij}\right)_{n\times n} \tag{6}$$

3) The sorting vector is obtained by using the Eq. (7).

$$W^{(0)}=\left(w_1,w_2,\cdots w_n\right)^T=\left[\frac{\sum_{j=1}^{n}e_{1j}}{\sum_{i=1}^{n}\sum_{j=1}^{n}e_{ij}},\frac{\sum_{j=1}^{n}e_{2j}}{\sum_{i=1}^{n}\sum_{j=1}^{n}e_{ij}},\cdots\frac{\sum_{j=1}^{n}e_{nj}}{\sum_{i=1}^{n}\sum_{j=1}^{n}e_{ij}}\right]^T \tag{7}$$

4) Use the conversion Eq. (8) to transform the Eq. (5) into a mutual form matrix obtion Eq. (9).

$$e_{ij}=\frac{r_{ij}}{r_{ji}} \tag{8}$$

$$E=\left(e_{ij}\right)_{n\times n} \tag{9}$$

5) The ranking vector $W^{(0)}$ serves as the initial estimate V_0 for the eigenvalue method. Through iterative calculation, the eigenvector V_{k+1} is derived (Eq. (11)), the infinite norm $\|V_{k+1}\|_\infty$ is calculated, and the maximum eigenvalue $\lambda_{\max}$ is determined. After normalization (Eq. (13)), the scheme ordering vector $W^{(k)}=V_{i+1}$ is obtained. If convergence is not reached, Eq. (14) is adopted as a new initial estimate, and the iteration continues.

$$V_0=V_0\left(v_{01},v_{02},\cdots v_{0n}\right)^T \tag{10}$$

$$V_{k+1}=EV_k \tag{11}$$

$$\|V_{k+1}\|_\infty-\|V_k\|_\infty<\varepsilon \tag{12}$$

$$V_{k+1}=\left[\frac{v_{k+1},1}{\sum_{i=1}^{n}v_{k+1},i},\frac{v_{k+1},2}{\sum_{i=1}^{n}v_{k+1},i},\cdots\frac{v_{k+1},n}{\sum_{i=1}^{n}v_{k+1},i}\right]^T \tag{13}$$

$$V_k=\frac{V_{k+1}}{\|V_{k+1}\|_\infty}=\left[\frac{V_{k+1},1}{\|V_{k+1}\|_\infty},\frac{V_{k+1},2}{\|V_{k+1}\|_\infty},\cdots\frac{V_{k+1},n}{\|V_{k+1}\|_\infty}\right]^T \tag{14}$$

6) As shown in Figure 3, expert scoring is used to evaluate multiple factors influencing floor water inrush [18]. Combined with Table 1, three priority judgment matrices corresponding to the three hierarchical levels of the 16$^{\text{th}}$ coal seam floor water inrush index system are established.

The comparison matrix for A-B is given below:

$$\begin{bmatrix}0.5 & 0.8 & 0.8 & 0.8\\ 0.2 & 0.5 & 0.6 & 0.7\\ 0.2 & 0.4 & 0.5 & 0.6\\ 0.2 & 0.3 & 0.4 & 0.5\end{bmatrix} \tag{15}$$

The comparison matrix for B_1-C is shown as follows:

$$\begin{bmatrix} 0.5 & 0.7 \\ 0.3 & 0.5 \end{bmatrix} \tag{16}$$

The comparison matrix for B_2-C is presented accordingly:

$$\begin{bmatrix} 0.5 & 0.6 \\ 0.4 & 0.5 \end{bmatrix} \tag{17}$$

The weights of each factor calculated by the IFAHP approach are listed in Table 3.

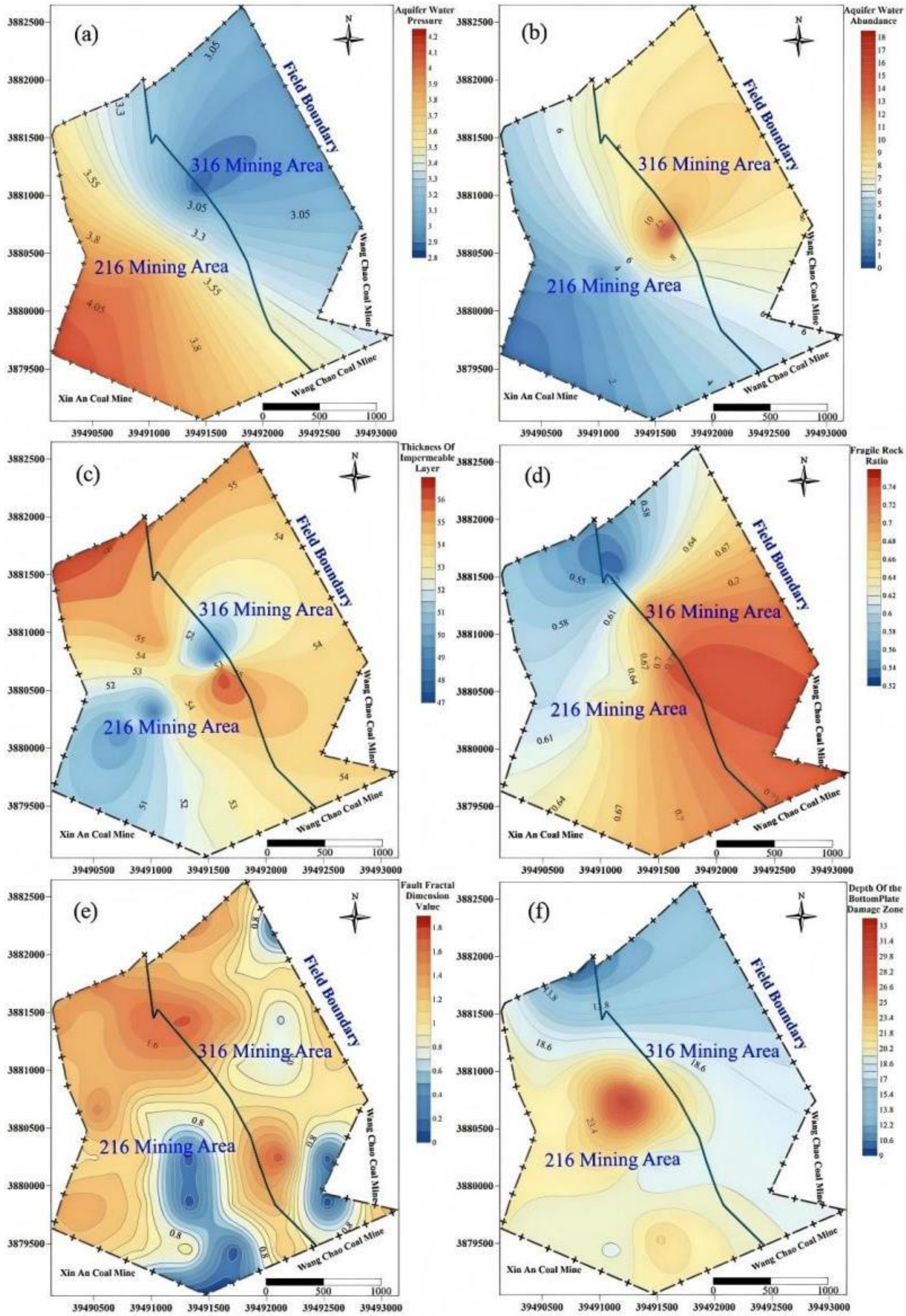

Figure 3 Thematic map of risk assessment index of water inrush in floor

Table 3 IFAHP determines the weight results of each master factor

Method of determining rights	Ordovician limestone water abundance (w_1^{α})	Ordovician limestone water pressure (w_2^{α})	Aquifuge thickness (w_3^{α})	Fragile rock ratio (w_4^{α})	Fault fractal dimension value (w_5^{α})	Floor failure depth (w_6^{α})
IFAHP	0.148	0.256	0.101	0.133	0.197	0.165
EWM	0.061	0.401	0.069	0.056	0.377	0.036
IFAHP-EWM	0.092	0.350	0.041	0.044	0.438	0.035

4.2 The Objective Weights Determined by EWM

The Entropy Weight Method (EWM), grounded in information theory, was applied to determine the objective weights of the evaluation indicators. In this framework, information quantifies the degree of system order, while entropy measures the level of uncertainty or disorder. This approach enables an objective assessment of each indicator's relative influence within the evaluation system, providing a robust basis for comprehensive analysis. An index with a lower entropy value contains more effective information and therefore has a greater influence on the overall assessment, resulting in a higher weight [19].

Taking the standardized matrix R with a evaluation objects and b evaluation indicators as the basis, and the entropy of the i-th factor e_i among the i influencing factors, as shown in Eq. (18). This provides a quantitative measure of the information contribution of each factor.

$$e_i = -\frac{1}{\ln a}\sum_{j=1}^{\alpha} P_{ij}\ln P_{ij} \tag{18}$$

where, P_{ij} represents the weight of the indicator value of the j-th evaluation object with respect to the i-th indicator.

$$P_{ij} = -\frac{X_{ij}}{\sum_j^{\alpha} X_{ij}} \tag{19}$$

Accordingly, he entropy weights of all indicators are obtained, serving as an objective reference for evaluation. The weight for the i-th indicator is expressed in Eq. (20):

$$W^{\beta}{}_i = \frac{1-e_i}{\alpha - \sum_{j=1}^{\alpha} e_i} \tag{20}$$

The weight of each factor obtained by EWM are listed in Table 3.

4.3 Comprehensive Weights Determined by IFAHP-EWM

The final comprehensive weights W are derived by integrating the subjective weights W^{α} obtained from IFAHP with the objective weights W^{β} obtained from EWM, as expressed in Eq. (21). The results of the entropy weight calculation for each factor are summarized in Table 3.

$$W_i = \frac{W_i^{\alpha} W_i^{\beta}}{\sum_{i=1}^{b} W_i^{\alpha} W_i^{\beta}} \tag{21}$$

5 Construction of the Dynamic Variable Weight Model

As floor water inrush is governed by multiple interrelated factors, their combined influence can significantly affect the overall risk. To more precisely capture the dynamic contribution of each factor, a variable weight function was incorporated, forming the foundation of a dynamic variable-weight model. This approach not only emphasizes the relative significance of the selected indicators but also accounts for their variability, thereby improving the accuracy and reliability of risk assessment.

5.1 Establish the Weight Vector of the State Variable

A state variable weight vector is formulated and partitioned into four functional intervals: the penalty interval, the neutral (non-incentive-non-penalty) interval, the initial incentive interval, and the strong incentive interval. The mathematical representation is provided in Eq. (22), while its functional curve is illustrated in Figure 4.

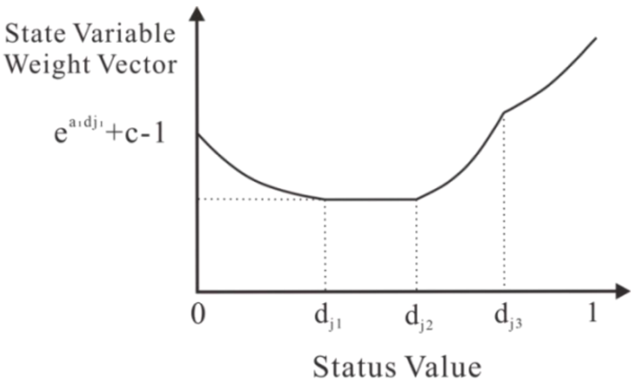

Figure 4 State variable weight vector diagram of different master factors

$$S(X)=(S_1(X),S_2(X),\cdots,S_n(X))$$

$$S_j(X)=\begin{cases} e^{a_1(d_{j1}-X)}+c-1, X\in[0,d_{j1}] \\ c, X\in[d_{j1},d_{j2}] \\ e^{a_2(X-d_{j2})}+c-1, X\in[d_{j2},d_{j3}] \\ e^{a_3(X-d_{j3})}+e^{a_2(d_{j3}-d_{j2})}+c-2, X\in[d_{j3},1) \\ (j=1,2,3,\cdots,n) \end{cases} \tag{22}$$

where, X is the factor state value; $S(X)$ is the n-dimensional partition state variable weight vector; $S_j(X)$ is the j-th element in the n-dimensional partition state variable weight vector; n is the number of influencing factors; c, a_1, a_2, and a_3 are the weight adjustment parameters; dj_1, dj_2, and dj_3 are the threshold values of the j-th variable weight interval.

5.2 Determine the Variable Weight Intervals of Evaluation Indices

K-means clustering analysis is employed to categorize the water inrush evaluation indicators for the 16th coal seam floor underlain by Ordovician limestone. Using the clustering centers of the key controlling factors, the threshold values of each indicator are identified, thereby defining their respective variable weight intervals. Accordingly, unified variable weight intervals—denoted by dj_1, dj_2, and dj_3 are defined and used to partition the evaluation indices, as shown in Table 4.

Table 4 Change weight interval of the evaluation index

Main control factors	**Change the right interval**			
	Penalty interval	**Non incentive non penalty interval**	**Initial incentive interval**	**Strong incentive interval**
Ordovician limestone water abundance	<0.350	0.350~0.505	0.505~0.660	>0.660
Ordovician limestone water pressure	<0.117	0.117~0.297	0.297~0.495	>0.495
Aquifuge thickness	<0.336	0.336~0.520	0.520~0.702	>0.702
Fragile rock ratio	<0.284	0.284~0.415	0.415~0.569	>0.569
Fault fractal dimension value	<0.158	0.158~0.419	0.419~0.648	>0.648
Floor failure depth	<0.329	0.329~0.477	0.477~0.593	>0.593

5.3 Confirm Weight Adjustment Parameters

Adjustment parameters (a_1, a_2, and a_3) are introduced to regulate the extent of weight variation for each control factor. The constraint weight and ideal weight variation of each main control factor indicator are determined by constructing an evaluation unit that satisfies. Four equations are established to solve for the four parameters. After repeated debugging and calibration, the final values are determined as: c=0.3, a_1=0.445, a_2=0.515, a_3=1.0358.

5.4 Construct a Variable Weight Model and Calculate the Weights and State Values of Evaluation Index

By integrating the state variable weight vector, defined variable weight intervals, and adjustment parameters, a comprehensive variable weight model is developed for the 16th coal seam floor. This model is then applied to the quantitative dataset of evaluation indicators, allowing the calculation of variable weights and state values for each evaluation unit.

$$W(X)=\frac{W^{c}\cdot S(X)}{\sum_{1}^{6}w_{j}^{c}S_{j}(X)}=\left(\frac{w_{1}^{c}S_{1}(X)}{\sum_{j=1}^{6}w_{j}^{c}S_{j}(X)},\frac{w_{2}^{c}S_{2}(X)}{\sum_{j=1}^{6}w_{j}^{c}S_{j}(X)},\cdots,\frac{w_{6}^{c}S_{6}(X)}{\sum_{j=1}^{6}w_{j}^{c}S_{j}(X)}\right)$$

$$S_{j}(X)=\begin{cases}e^{0.445(d_{j1}-X)}+0.3-1, X\in[0,d_{j1})\\ 0.3, X\in[d_{j1},d_{j2})\\ e^{0.5156(X-d_{j2})}+0.3-1, X\in[d_{j2},d_{j3})\\ e^{1.0358(X-d_{j3})}+e^{0.515(d_{j3}-d_{j2})}+0.3-2, X\in[d_{j3},1)\end{cases} \tag{23}$$

$$(j=1,2,3,\cdots,6)$$

where, $W(X)$ is the variable weight vector; dj_1, dj_2, and dj_3 are the variable weight interval thresholds for the j-th main control factor; W_c is a constant weight vector.

For various factors: $W^{c}=(w_{1}^{c},w_{2}^{c},w_{3}^{c},\cdots,w_{6}^{c})$; $w_{1}^{c},w_{2}^{c},w_{3}^{c},\cdots,w_{6}^{c}$. The quantitative database of indicators is processed through the variable weight model to compute the variable weights for each evaluation unit.

6 Model Application and Risk Zoning

6.1 Establish the Evaluation and Prediction Model

The water inrush index was obtained by calculating each index using the linear weighting method, and the calculation process is shown in Eq. (24):

$$N=C_{1}w_{1}+C_{2}w_{2}-C_{3}w_{3}-C_{4}w_{4}+C_{5}w_{5}+C_{6}w_{6} \tag{24}$$

Where, N is the water inrush index; C_1, C_2, C_3, C_4, C_5, and C_6 is the standardized data for each factor; w is the weights after variable weighting within different ranges.

6.2 Results and Discussions

The dynamic weight model was applied to calculate the floor water inrush index and establish a corresponding risk assessment framework for the Ordovician limestone aquifer. The standardized dataset of the 16th coal seam was input into the model to derive index values for each evaluation unit, revealing the spatial distribution pattern of water inrush risk. Based on predefined thresholds, the coal seam floor was classified into four zones within a GIS environment: Safe (I), Relatively Safe (II), Relatively Hazardous (III), and Hazardous (IV), and a zoning map was produced accordingly (Figure 5a). The results were also compared with those obtained from the constant-weight model (Figure 5d).

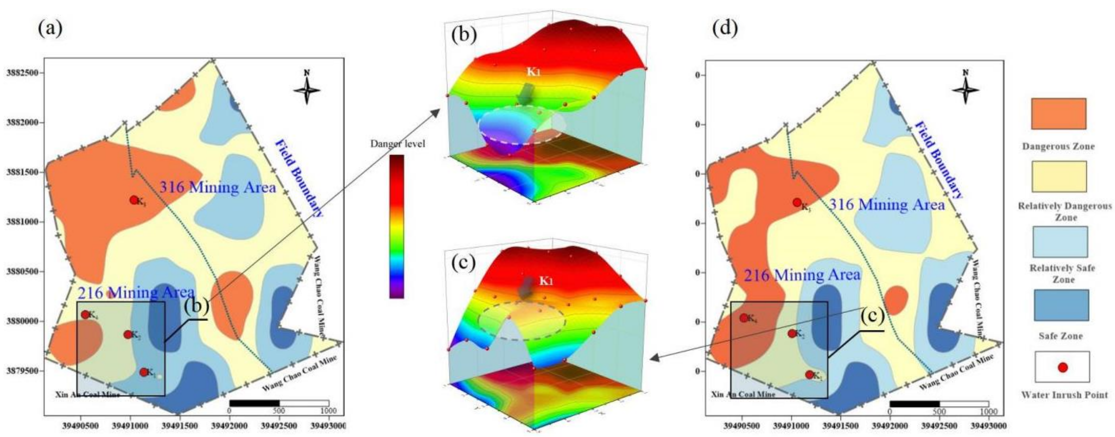

Figure 5 Integrated zoning maps of water inrush risk based on subjective-objective multi-source data coupling

(a) dynamic variable weight evaluation; (b) constant weight evaluation 3D visualization of risk distribution; (c) dynamic variable weight evaluation 3D visualization of risk distribution; (d) constant weight evaluation

To validate the model, documented water inrush events from mined-out areas were superimposed on the zoning map. Statistical analysis indicates that 82% of the recorded inrush points fall within Zones III and IV, demonstrating strong agreement between model predictions and actual occurrences. Notably, the IFAHP-EWM-based dynamic model correctly identified the K_1 and K_4 inrush points as Hazardous and Relatively Hazardous, respectively, whereas the constant-weight model underestimated their risk levels. This confirms that the dynamic weight model provides more precise and reliable risk zoning.

Furthermore, a 3D visualization was constructed to illustrate the spatial variation of the inrush index and highlight the clustering characteristics of hazardous areas (Figure 5c, 5d). The integration of the 2D zoning map with the 3D visualization enhances understanding of the spatial pattern and development of water inrush risk.

In summary, the zoning results and 3D visualization collectively verify the improved predictive performance of the proposed IFAHP-EWM dynamic weighting model. The method offers a practical and theoretically robust framework for early warning and prevention of floor water inrush, and targeted control measures are recommended for high-risk zones.

7 Conclusions

1) According to the measured data, the existing literature research results, and the related studies on the influencing factors of floor water inrush, an evaluation index structure model was established by selecting six evaluation indexes: AWP, AWA, AT, FRR, FFDV, FFD. A thematic map of floor water inrush risk evaluation index is drawn.
2) The weights were obtained separately using the IFAHP and EWM methods, and then integrated to derive comprehensive weights. A variable weight function was introduced to construct a state variable weight vector consisting of four intervals. K-means clustering was applied to partition the variable weight intervals, and suitable adjustment parameters were determined through calculation and fine-tuning. On this basis, a variable weight model was developed for risk evaluation.
3) The risk of water inrush from the Ordovician limestone underlying the study area was categorized into four levels: Safe (I), Relatively Safe (II), Relatively Hazardous (III), and Hazardous (IV). Accordingly, a risk zoning map of the 16th coal seam floor was generated. Validation against known water inrush events, together with comparison to the constant-weight model and three-dimensional visualization, demonstrates that the proposed dynamic variable weight model produces more accurate and realistic predictions. This work provides theoretical guidance for the safe extraction of coal seams and highlights the necessity of implementing effective water-control measures in hazardous zones during future mining operations.

Ethical Approval

This article does not contain any studies with human participants or animals performed by any of the authors.

Authors Statement

All authors contributed to the study conception and design. Writing-review, editing and Supervision were performed by Yanlei Li. The first draft of the manuscript was written by Shuzhen Tai. Formal analysis and Software were performed by Yongjie Li, Lifeng Zhang. Data curation was performed by Xinfeng Li, Chao Liu. Investigation and Project administration were performed by Huiyong Yin, Guoliang Xu, Fangying Dong. All authors read and approved the final manuscript.

Data Availability

The datasets used and analyzed during the current study are available from the corresponding author on reasonable.

Conflicts of Interest

The authors declare that they have no known competing financial interests or personal relationships that could have appeared to influence the work reported in this paper.

References

[1] Cao, Y. Q., 1997. Research on the basic theory of floor water bursting and water prevention and control principle in mining face. Jour Geol & M in Res North China, 1997(03): 19-20.

[2] Sun, W. J., Wang, Y. W., Li, X. K., Yang, W. K., He, Y. C., Wu, F. H., 2015. Analysis on Hydrogeological Classification and Water Inrush Accidents in North China Coal Mines. Coal Engineering, 2015, 47(06): 103-105. https://doi.org/10.11799/ce201506033

[3] Zhao, Q. B., Zhao, B. W., Fu, Y. G., Nan, S. H., Zhao, Z., 2016. Research on key technology to control Ordovician limestone water disaster on surface region of deep mining depth mine. Coal Science and Technology, 2016, 44(08): 14-20. https://doi.org/10.13199/j.cnki.cst.2016.08.003

[4] Liu, Q. M., Hu, J. W., 2011. Research on method of water-resisting coefficient for distinguishing floor water inrush danger. Procedia Earth and Planetary Science, 2011, 3: 238-245. https: //doi.org/10.1016/j.proeps.2011.09.089

[5] Wu, Q., Fan, Z. L., Liu, S. Q., Zhang, Y. W., Sun, W. J., 2011. Water-richness evaluation method of water-filled aquifer based on the principle of information fusion with GIS: Water-richness index method. Journal Of China Coal Society, 2011, 36(7): 1124-1128. https://doi.org/10.13225/j.cnki.jccs.2011.07.002

[6] Hou, E. K., Ji, Z. C., Che, X. Y., Wang, J. W., Gao, L. J., Tian, S. X., Yang, F., 2019. Water abundance prediction method of weathered bedrock based on improved AHP and the entropy weight method. Journal of China Coal Society, 2019, 44(10): 3164-3173. https://doi.org/10.13225/j.cnki.jccs.2018.1210

[7] Shi, L. Q., Zhang, R. A., Xu, D. J., 2020. Prediction of water inrush from floor based on GWO-Elman neural network. Journal Of China Coal Society, 2020, 45(07): 2455-2463. https://doi.org/10.13225/j.cnki.jccs.DZ20.0716

[8] Li, Z. J., 2010. Comprehensive Evaluation of Water-inrush Risk from Coal Floor by Both Water-inrush Coefficient and Fuzzy Cluster Methods. Mining Safety & Environmental Protection, 2010(1): 3. https://doi.org/10.3969/j.issn.1008-4495.2010.01.009

[9] Dong, F. Y., Yin, H. Y., Cheng, W. J., Li, Y. J., Qiu, M., Zhang, C. W., Tang, R. Q., Xu, G. L., Zhang, L. F., 2022. Study on water inrush pattern of Ordovician limestone in North China Coalfield based on hydrochemical characteristics and evolution processes: a case study in Binhu and Wangchao Coal Mine of Shandong Province, China. Journal of Cleaner Production. 380, 134954. https://doi.org/10.1016/j.jclepro.2022.134954

[10] Dong, J. X., Shen, Z. L., Cao, L., Mi, J., Li, J. G., Zhao, Y. C., Mu, H. Y., Liu, L. P., Dai, C. R., 2023. Water-sand inrush risk assessment method of sandy dolomite tunnel and its application in the Chenaju tunnel, southwest of China, Geomatics, Natural Hazards and Risk, 14: 1, https://doi.org/10.1080/19475705.2023.2196369

[11] Xiao, L. L., Wu, Q., Niu, C., Dai, G. L., Wang, S. Q., Ren, D. J., Luo, S. T., 2020. Application of a new evaluation method for floor water inrush risk from the Ordovician fissure confined aquifer in Xiayukou coal mine, Shanxi, China. Carbonates and Evaporites, 2020, 35: 1-16. https://doi.org/10.1007/s13146-020-00629-x

[12] Guo, Y. R., Dong, S. N., Hao Y. H, Liu, Z. B., Chyi Jim Yeh, T., Wang, W. K., Gao, Y. Q., Li, P., Zhang, M., 2020. Risk assessments of water inrush from coal seam floor during deep mining using a data fusion approach based on grey system theory. Complexity, 2020, 2020: 1-12. https://doi.org/10.1155/2020/8205370

[13] Chen, Y. F., Chen, L. W., Peng, Z. H., Zhang, M., Hu, Y. S., Oua, Q. H., Zhang, J., Tian, Y., Shi, X. P., 2023. An improved model to predict the water-inrush risk under an unconsolidated confined aquifer based on analytic hierarchy process and information value method, Geomatics, Natural Hazards and Risk, 14: 1, https://doi.org/10.1080/19475705.2023.2236277

[14] Yin, S. X., Wu, Z. Y., 2019. Quantitative Evaluation of Structural Complexity of Qianjiaying Mine Field. Safety In Coal Mines, 2019, 50(05): 218-221. https://doi.org/10.13347/j.cnki.mkaq.2019.05.053

[15] Zheng, Y. M., Wang, Y. D., Sun, H., Ge, X. R., 2022. Embankment Stability Evaluation Based on Improved FAHP. Journal of Gansu Sciences, 2022, 34(4): 91-97. https://doi.org/10.16468/j.cnki.issn1004-0366.2022.04.015

[16] Jiskani, I. M, Shah, S. A. A., Cai, Q. X., Zhou, W., Lu, X., 2020. A multi-criteria based SWOT analysis of sustainable planning for mining and mineral industry in Pakistan. Arabian Journal of Geosciences, 2020, 13: 1-16. https://doi.org/10.1007/s12517-020-06090-3

[17] Zhao, B. X., Liu, Q. M., Zhu, J. Z., 2023. Risk Assessment and Zonation of Roof Water Inrush Based on the Analytic Hierarchy Process, Principle Component Analysis, and Improved Game Theory (AHP-PCA-IGT) Method. Sustainability, 2023, 15(14): 11375. https://doi.org/10.3390/su151411375

[18] Zhang, H., Wu, Q., 2020. Application of constant weight vulnerability index method of water-inrush from coal seam floor based on entropy method and FAHP. China Energy and Environmental Protection, 2020, 42(4): 1-5, 9. https://doi.org/10.19389/j.cnki.1003-0506.2020.04.001

[19] Liu, S. Q., Wu, Q., Li, Z., 2021. Vulnerability evaluation and application of floor water inrush in mining area withmultiple coal seams and single aquifer based on variable weight. Journal of China University of Mining &. Technology 2021 50(3): 587-597. https://doi.org/10.13247/j.cnki.jcumt.001290